Pictorial Essay | Gastrointestinal Imaging

eISSN 2005-8330
https://doi.org/10.3348/kjr.2019.0774
Korean J Radiol 2020

Korean Journal of Radiology
KJR

MR Imaging of the Perihepatic Space

Angèle Bonnin, MD[1], Carole Durot, MD[1], Manel Djelouah, MD[1], Anthony Dohan, MD, PhD[2, 3], Lionel Arrivé, MD, PhD[4], Pascal Rousset, MD, PhD[5, 6], Christine Hoeffel, MD, PhD[1, 7]

[1]Department of Radiology, Centre Hospitalo-Universitaire de Reims, Reims, France; [2]Department of Abdominal and Interventional Radiology, Hôpital Cochin, Assistance Publique-Hôpitaux de Paris, APHP, Paris, France; [3]Paris Descartes University, Sorbonne Paris-Cité-Paris V, Paris, France; [4]Department of Radiology, Saint-Antoine Hospital, Assistance Publique-Hôpitaux de Paris, Sorbonne Université, Paris, France; [5]Department of Radiology, Hospices Civils de Lyon, Centre Hospitalier Lyon Sud, Pierre Bénite, France; [6]Lyon 1 Claude Bernard University, Lyon, France; [7]CRESTIC, Reims Champagne-Ardenne University, Reims, France

The perihepatic space is frequently involved in a spectrum of diseases, including intrahepatic lesions extending to the liver capsule and disease conditions involving adjacent organs extending to the perihepatic space or spreading thanks to the communication from intraperitoneal or extraperitoneal sites through the hepatic ligaments. Lesions resulting from the dissemination of peritoneal processes may also affect the perihepatic space. Here we discuss how to assess the perihepatic origin of a lesion and describe the magnetic resonance imaging (MRI) features of normal structures and fluids that may be abnormally located in the perihepatic space. We then review and illustrate the MRI findings present in cases of perihepatic infectious, tumor-related, and miscellaneous conditions. Finally, we highlight the value of MRI over computed tomography.
Keywords: *Magnetic resonance imaging; Liver; Computed tomography; Peritoneum*

INTRODUCTION

The perihepatic space is composed of different spaces, mainly the right subphrenic and subhepatic spaces. The liver is surrounded by the visceral peritoneum, which usually contains a small amount of serous fluid. The spread of inflammatory and tumoral processes to the perihepatic space is dependent on the distribution and dynamics of the peritoneal fluid. The latter is determined by hydrostatic pressure and the effect of gravity as well as peritoneal recesses and mesenteric reflections. Liver disease conditions may also extend to the liver capsule and subsequently to the perihepatic space. Extension from other peritoneal or extraperitoneal sites may follow the communication pathways through the hepatic ligaments to the perihepatic space (1).

Computed tomography (CT) is the usual cross-sectional imaging technique with which the perihepatic space abnormalities are discovered and evaluated. However, as magnetic resonance imaging (MRI) is being used more widely, it is crucial to be familiar with the appearance of these lesions on MRI. Moreover, the optimal contrast resolution of MRI allows better detection and characterization of some lesions in the perihepatic space compared to CT.

The purpose of this article was to describe the MRI characteristics of abnormalities of the perihepatic space and highlight and illustrate the value of MRI over CT in this setting.

Anatomic Considerations

The liver is surrounded by the Glisson capsule, an extrusion of the visceral peritoneum, except for the bare area, which is attached to the diaphragm. The suspensory ligaments of the liver include the coronary ligaments, the triangular ligaments, and the falciform ligament.

The falciform ligament, composed of a double fold of

Received: March 18, 2019 **Revised:** May 2, 2020
Accepted: June 23, 2020
Corresponding author: Angèle Bonnin, MD, Department of Radiology, Centre Hospitalo-Universitaire de Reims, 45 rue Cognac Jay, Reims 51092, France.
• E-mail: abonnin@chu-reims.fr

peritoneum (1) and containing the obliterated umbilical vein, connects the anterior abdominal wall and the diaphragm to the liver. This ligament separates segments 2 and 3 from segment 4 (Fig. 1A). The falciform ligament forms a partial barrier between the right and left subphrenic space yet allows the transfer of fluid from one side to the other. The inferior part of the falciform ligament is elongated by the Teres ligament.

The coronary ligament, contiguous with the falciform ligament and composed of left and right ligaments, is the largest attachment of the liver to the diaphragm. The triangular ligaments are formed by fusion of inferior and superior reflections of the coronary ligaments. The left triangular ligament is short and does not compartmentalize the left subphrenic space, unlike the right triangular ligament, which is long and separates the right subphrenic space from the right subhepatic space (2).

The lesser omentum is divided into two parts: the gastrohepatic and the hepatoduodenal ligaments. The gastrohepatic ligament connects the lesser curve of the stomach to the liver and contains the coronary vein and left gastric artery. The hepatoduodenal ligament connects the duodenum to the liver and hosts the portal vein, hepatic artery, common hepatic duct, and part of the cystic duct.

The subhepatic space is divided into an anterior and a posterior space. The anterior subhepatic space is located posteriorly to the portal vein and freely communicates with the lesser sac via the Winslow foramen (3). The posterior subhepatic space is known as the Morison's pouch and is contiguous with the anterior right Gerota fascia (4). The perihepatic space includes the right subphrenic space, the subhepatic space, the lesser sac, and the left perihepatic space.

Peritoneal disease extends to the perihepatic space in a clockwise direction through the right paracolic gutter to the Morrison's pouch and the right subphrenic space. Right subphrenic pathology can spread to the left subphrenic space and anterior wall. Hepatobiliary disease can spread to the perihepatic space and peritoneum through the falciform ligament. The hepatoduodenal ligament constitutes a route for the spread of pancreatic disease to the porta hepatis and liver (Fig. 1B).

The anatomy, as described above, is presented in an animated picture (Supplementary Video 1).

Assessing the Perihepatic Origin of a Lesion

Assessing the perihepatic origin of a lesion versus its intrahepatic origin presents a major challenge, particularly when the lesion is large. It may be straightforward when the tumor is completely surrounded by liver parenchyma, indicating that it is intrahepatic, when the liver parenchyma is compressed and displaced, and when there is a fat layer between the tumor and the liver parenchyma indicating its extrahepatic origin. In other situations, other signs may be helpful such as identifying an arterial supply to a pedunculated tumor originating from the hepatic arteries, which suggests an intrahepatic location of the tumor. Identifying the tumor center may also suggest that the tumor is probably extrahepatic when the center is outside

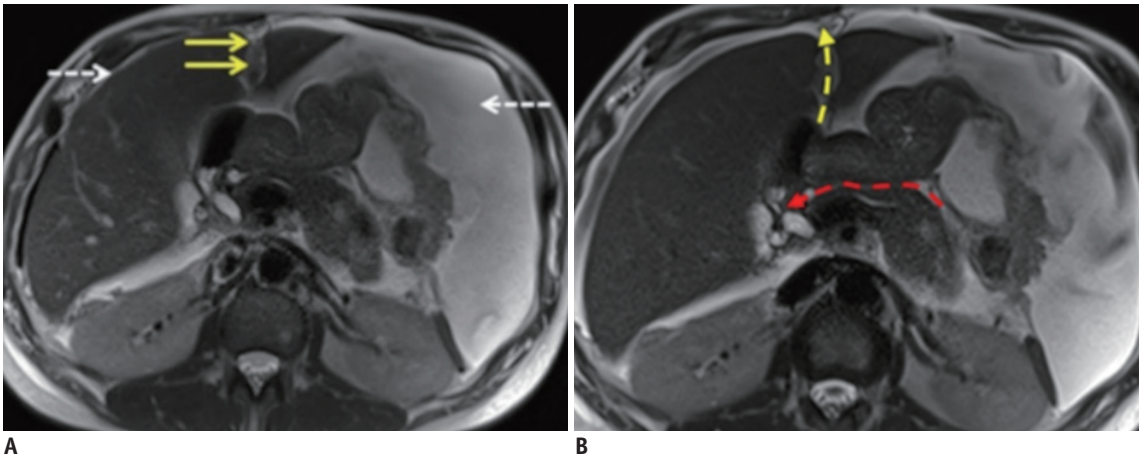

A B

Fig. 1. Anatomy of the perihepatic space.
Falciform ligament (yellow arrows, **A**) separates the left and right hepatic lobes, and the right from the left subphrenic space (dashed arrows). On axial T2-weighted MR images **(B)** shows the spread of hepatobiliary disease to the perihepatic space and peritoneum through the falciform ligament (yellow arrow). Pancreatic and gastric disease spread to the porta hepatis and liver through the lesser omentum (red arrow). MR = magnetic resonance

https://doi.org/10.3348/kjr.2019.0774

Korean Journal of Radiology
KJR

the liver. Some signs may help differentiate between right hepatic and right retroperitoneal lesions. Large tumors, such as those found in the inferior vena cava or the right portal bifurcation, may displace the vessels. A large tumor arising from the right liver can increase the distance between the right anterior and the right posterior portal branches, while large extrahepatic tumors displace vessels differently. For example, a large adrenocortical carcinoma will displace the inferior vena cava and the portal branches anteriorly and clockwise. A summary is displayed in an animated picture (Supplementary Video 2).

Unusual Perihepatic Location of Normal Structures or Fluids

Structures Abnormally Located in the Perihepatic Space

The intestines, mainly the colon, may interpose temporarily or permanently between the liver and the diaphragm, which is known as Chilaiditi syndrome (5). Usually, it is an asymptomatic and incidental imaging finding. The gallbladder may very rarely be found wandering in a perihepatic position, even in the absence of acute volvulus in elderly persons. Varices may also be found around the liver as a consequence of portal hypertension.

Fat may be found, although rarely, medially and adjacent to the lumen of the inferior vena cava, near the hepatic confluence. Lastly, the omentum may be used as packing material in hepatobiliary surgery, which then appears as a fatty mass in the perihepatic space (6).

Abnormal Location of Fluids

Perihepatic fluid collection may result from accumulation of ascites, blood, bile, chyle, pancreatic necrosis, or urine. MRI, due to its high-contrast resolution, may allow a better depiction of hemorrhagic content than CT and may thus provide a more precise definition of the location of a lesion. Perihepatic fluids are hypointense on T1-weighted images, even during the hepatobiliary phase.

Conversely, bile leaking into the perihepatic fluid will appear as a high signal intensity on late enhanced T1-weighted sequences after intravenous administration of specific hepatobiliary contrast agents (Fig. 2) (7). However, it has been shown that peritoneal fluids may display a signal intensity that increases progressively over time, even in the absence of any biliary leakage on T1-weighted gradient-echo sequences after injection of gadobenate dimeglumine (Gd-BOPTA) (8).

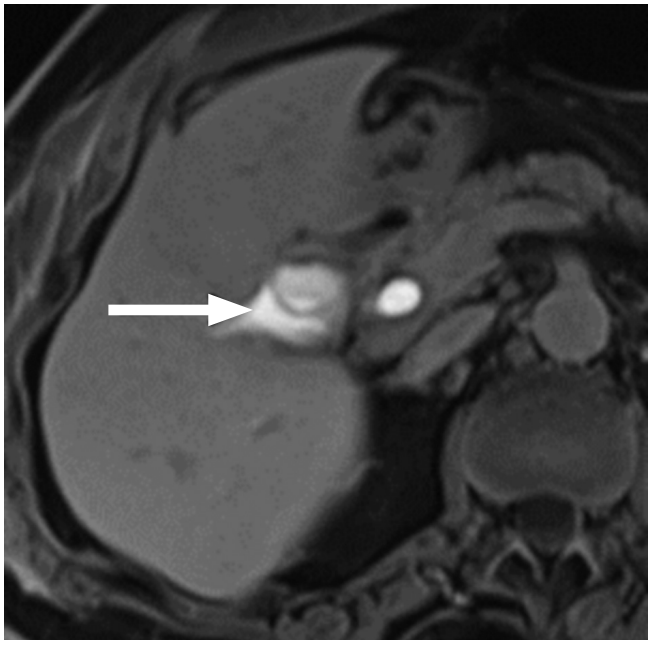

Fig. 2. Biliary leakage post-cholecystectomy. A 69-year-old female ten days after a cholecystectomy complicated by fluid collection drained under radiological guidance. Axial T1-weighted sequence one and a half hours after intravenous administration of gadobenate dimeglumine shows high-signal intensity fluid seen in the hepatic hilum (arrow), confirmed the bilious nature of the leak.

CT is the most frequently used imaging technique for assessment and follow-up of acute pancreatitis and collections. MRI is an appropriate alternative for the characterization of fluid collections, particularly solid debris and fat necrosis (9). Pseudocysts and acute necrotic collections are usually peripancreatic, but they may occasionally be located in the perihepatic space (10, 11).

Disease Conditions

The clinical presentation and treatment of the different disease conditions that may involve the perihepatic space are listed in Table 1.

Infection

Stone-Related Perihepatic Abscesses

Depending on peritoneal anatomy and pressure gradients, abdominal infections are more likely to extend to the right side than to the left, and the perihepatic space, mainly the retrohepatic space, is regularly involved. Small foreign bodies, such as stercoliths left behind after an appendectomy, or dropped gallstones after a cholecystectomy, may get trapped in the perihepatic space, with subsequent formation of an abscess (12). The latter

 https://doi.org/10.3348/kjr.2019.0774

Table 1. Clinical Presentation and Treatment of the Different Perihepatic Disease

Perihepatic Space Abnormality	Symptoms and Clinical Examination	Treatment
Dropped stones-related perihepatic abscess	- History of cholecystectomy or appendectomy - Tenderness and pain in right upper quadrant - Fever - Elevated white blood cell count	- Antibiotic therapy - Surgical removal of stones
Echinococcosis	- Cholestatic jaundice and epigastric/right upper quadrant pain - Cholangitis - Portal hypertension and biliary cirrhosis from invasion of bile ducts and hepatic blood vessels	- Anthelmintic drugs
Tuberculosis	- Abdominal pain - Weight loss - Anemia - Fever with night sweats	- Antibiotic therapy
Perihepatic peritoneal metastases/ pseudomyxoma peritonei	- Imaging discovery unless large palpable mass	- Cytoreductive surgery
Diffuse peritoneal leiomyomatosis and fibromatosis	- Incidental discovery	- Surgery if necessary
Splenosis	- History of spleen trauma - Fortuitous discovery	- Absence
Fitz-Hugh-Curtis syndrom	- Sudden onset of right upper quadrant pain - Pelvic inflammatory disease	- Symptomatic - Treatment of primary infectious involvement
Endometriosis	- Diffuse or basithoracic pain during menses - Scapular or cervical pain - Catamenial pneumothorax - Pelvic endometriosis context	- Abdomen surgery - Thoracic surgery if recurrent catamenial pneumothorax
Intra-peritoneal focal fat infarction	- Abdominal pain and tenderness correlating with the location of the infarcted focal fat infarction	Conservative treatment

are generally small and discovered up to several years after the operation. They are increasingly being found owing to the development of laparoscopic procedures and may result in iterative febrile flareups whose origins are often underdiagnosed (13, 14).

Although CT is often sufficient for the detection of stercoliths, it may not always show a dropped gallstone with pure cholesterol content (Fig. 3). Unlike CT, MRI can detect all types of stones, even those that are small or non-calcified. Stones appear as hyperintense foci on T1-weighted images or as small hypointense abnormalities on both T1- and T2-weighted sequences.

Echinococcosis

Echinococcosis is a parasitic infection caused by the larva of the tapeworm Echinococcus. The two main forms include cystic hydatid disease (*Echinococcus granulosus*) and the less frequent alveolar hydatid disease (*Echinococcus multilocularis*). In both these forms, a cyst may rupture in the perihepatic space (15-17).

MRI is the best imaging technique for characterizing these lesions and defining their extension, both intra and extrahepatically, particularly to the subdiaphragmatic area and hepatic hilum. It best shows the multivesicular cystic structure of a lesion, depicted as areas of high T2 signal intensity (Fig. 4) (18). In both forms of echinococcosis, diagnosis is confirmed by specific serum antibodies detected in blood and confirmed by immunoassay.

Tuberculosis

Abdominal tuberculosis, although very rare, is increasingly encountered, even in developed countries. Hepatic and peritoneal involvement is usually seen with active thoracic tuberculous infection. However, the occurrence of isolated perihepatic tuberculosis with small abscesses in the perihepatic space has been described, although the exact mechanism remains unclear (19).

https://doi.org/10.3348/kjr.2019.0774

Korean Journal of Radiology
KJR

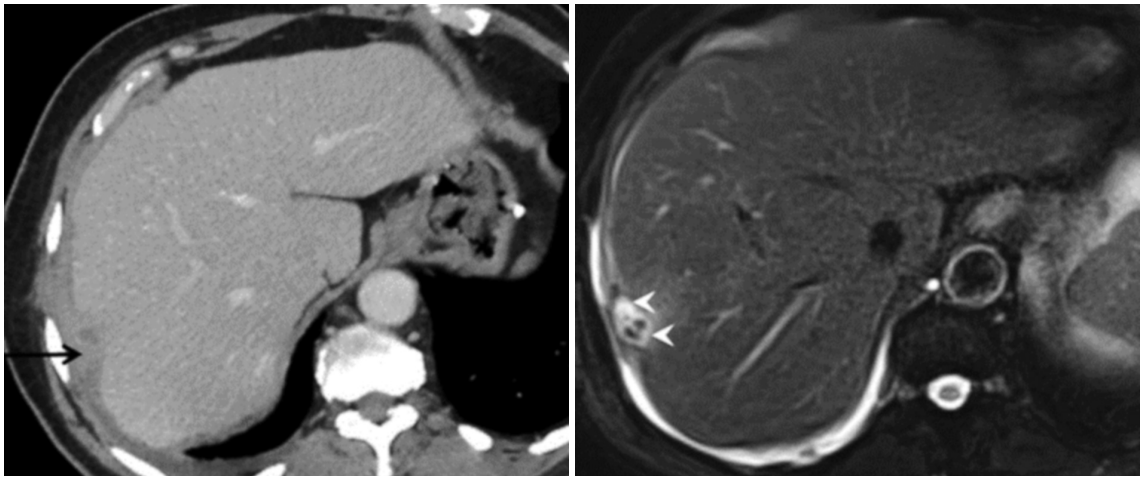

A B

Fig. 3. Abscess related to dropped gallstone. A 76-year-old male, heavy smoker, was referred to the hospital two months after a subtotal cholecystectomy performed for cholecystitis. He presented with fatigue and marked recent weight loss.
A. Axial portal venous phase CT image shows a perihepatic, nodular, hypoattenuating lesion, associated with perihepatic, focal, peritoneal thickening, suggestive of peritoneal metastasis (arrow). **B.** Axial fat-suppressed T2-weighted MR image reveals a small perihepatic abscess (arrowheads) with foci of signal loss indicating tiny gallstones that were not seen on CT. CT = computed tomography

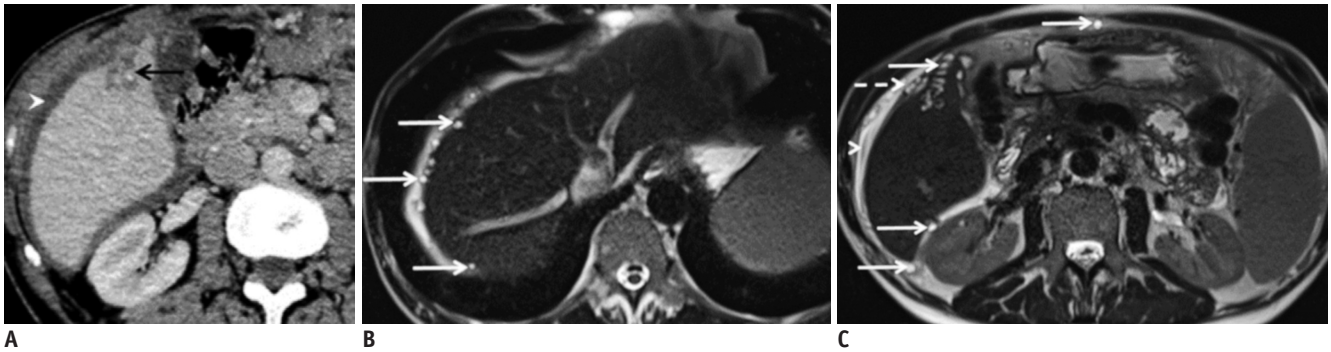

A B C

Fig. 4. Alveolar echinococcosis ruptured in the peritoneum. A 61-year-old male patient presenting with diarrhea for six months without any weight loss and mild abdominal pain. He had been eating lettuce from his garden in the countryside.
A. Axial contrast-enhanced CT slices show partially calcified cystic lesions in the liver (arrow) and peritoneal fluid (arrowhead). **B, C.** Axial HASTE T2-weighted MR images confirm the abnormalities seen on CT and show microvesicules floating in the peritoneal fluid (arrows) around the liver and thickened peritoneum (arrowhead). These findings are related to the intraperitoneal rupture of a microcystic alveolar echinococcosis lesion in the right liver (dashed arrow) with subsequent peritonitis.

Tumoral Involvement: Perihepatic Carcinomatosis and Its Mimics

Tumoral involvement of the perihepatic space may occur as an extrahepatic extension of a malignant liver lesion, but also as dissemination from a tumor located elsewhere via the lymphatic route or from being spread to the peritoneal space (e.g., from the undersurface of the diaphragm or Morison's pouch).

Perihepatic Peritoneal Metastases

CT and MRI features of perihepatic carcinomatosis include thickening, nodules, or masses in the peritoneum around the liver. Moreover, peritoneal enhancement after contrast medium intravenous administration may be abnormal in perihepatic peritoneal carcinomatosis. This enhancement is optimally detected five minutes after contrast medium injection. The subphrenic space is commonly involved, particularly on the right side, because of the preferential flow of peritoneal fluid into this space from the right paracolic gutter. Disease in this space is best depicted on contrast-enhanced reformatted coronal and sagittal MRI. MRI is very sensitive to small volumes of peritoneal carcinomatosis, showing thin peripheral lines of enhancement adjacent to the liver.

MRI may improve the detection of carcinomatosis, thus

 https://doi.org/10.3348/kjr.2019.0774

facilitating the diagnosis of this disease condition and help in the evaluation of the peritoneal carcinomatosis index (20, 21). The advantages of MRI are related to its superior contrast resolution and diffusion-weighted MRI, which allows detection and characterization of carcinomatosis nodules, particularly in the round ligament fossa and the hepatic hilum (Figs. 5, 6) (22-24).

Pseudomyxoma Peritonei

Pseudomyxoma peritonei (PMP) is characterized by the presence of a large amount of mucin in the abdomen due to neoplastic mucin-secreting cells, typically from an appendiceal primary tumor. MRI features include signs like those seen in peritoneal carcinomatosis. However, the high signal on T2-weighted MRI, the extent to which scalloping is present, the loculation of the peritoneal effusions, the predominance of lesions in the perihepatic space, and involvement of the greater omentum. At the same time, the gastrointestinal tract is rarely involved, signs highly suggestive of PMP (20, 25).

The assessment of perihepatic involvement, especially that of the hepatic pedicle, lesser omentum, and hepatoduodenal ligament infiltration, is crucial, as these sites are associated with incomplete cytoreductive surgery (25). MRI, due to its superior contrast resolution, both with T2, diffusion, and gadolinium-enhanced T1-weighted

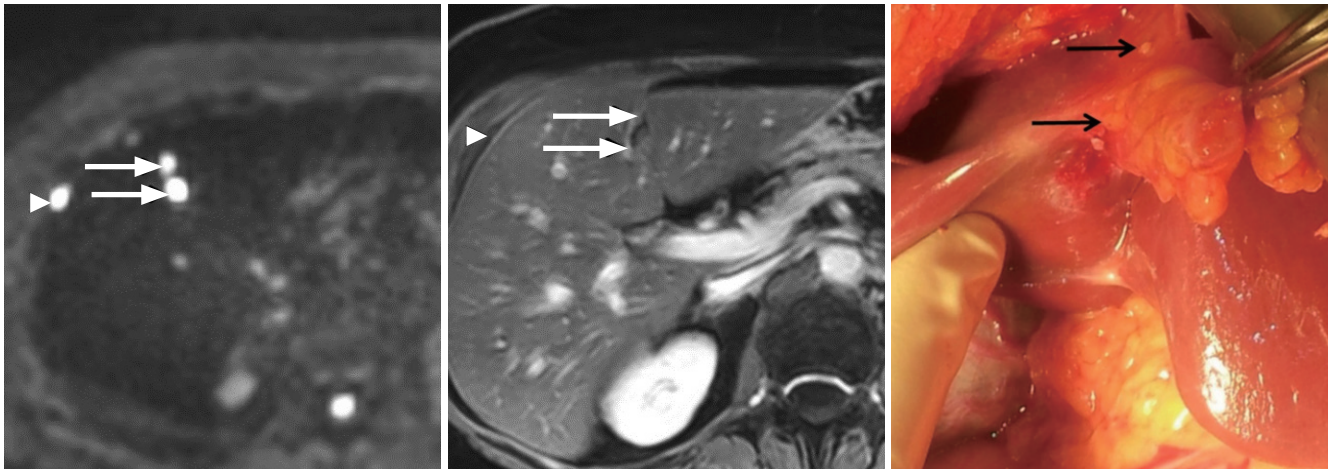

Fig. 5. Peritoneal metastases of a low-grade serous adenocarcinoma.
A 63-year-old female treated for low-grade serous adenocarcinoma with peritoneal metastases. Axial high b value diffusion-weighted MR image **(A)** optimally depicts the metastatic peritoneal implants of the perihepatic space, of the subphrenic space (arrowhead), and the implants located on both sides of the falciform ligament (arrows). These lesions are less easily detected and seen only in retrospect on axial gadolinium-enhanced MR **(B)** images (arrows and arrowhead). Intraoperative photograph **(C)** shows the lesions in the subphrenic space (arrows).

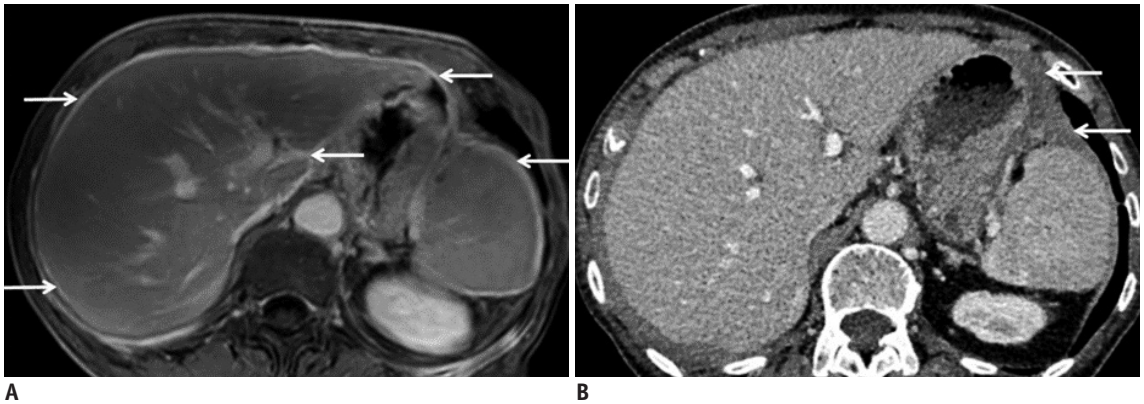

Fig. 6. Peritoneal metastases of an ovarian serous adenocarcinoma. Preoperative evaluation in a 66-year-old female with peritoneal recurrence of a moderately differentiated ovarian serous adenocarcinoma.
A. Axial fat-suppressed gadolinium-enhanced T1-weighted MR image optimally shows the enhancement and thickening of both the visceral and parietal layers of the perihepatic peritoneum along with the diaphragmatic cupola, Glisson's sheath, the lesser omentum, and the ductus venosus (arrows). These lesions were confirmed during laparotomy, thus jeopardizing curative resection. **B.** The peritoneal thickening is barely visible on the corresponding contrast-enhanced axial CT image, although CT was performed on the same day as the MRI (arrows). MRI = magnetic resonance imaging

https://doi.org/10.3348/kjr.2019.0774

Korean Journal of Radiology
KJR

sequences, allows improved detection and characterization of the perihepatic space, particularly when involvement is subtle or doubtful (Figs. 7, 8).

Diffuse Peritoneal Leiomyomatosis and Fibromatosis

Diffuse peritoneal leiomyomatosis findings include peritoneal nodules with histologic features similar to those of uterine leiomyomas (26). Malignant transformation is rare. MRI may have added value compared to CT for the characterization of homogeneous well-delineated soft-tissue perihepatic nodules, showing small well-delineated regular peritoneal nodules displaying low signal intensity on T2-weighted images and intermediate signal intensity on T1-weighted images. The nodules are homogeneously enhanced after intravenous administration of gadolinium chelates. Peritoneal fibromas are even rarer (Fig. 9).

Miscellaneous

Splenosis due to Implantation of Splenic Fragments

Most splenic implantations into the peritoneal cavity are found after a trauma to the spleen that has required a

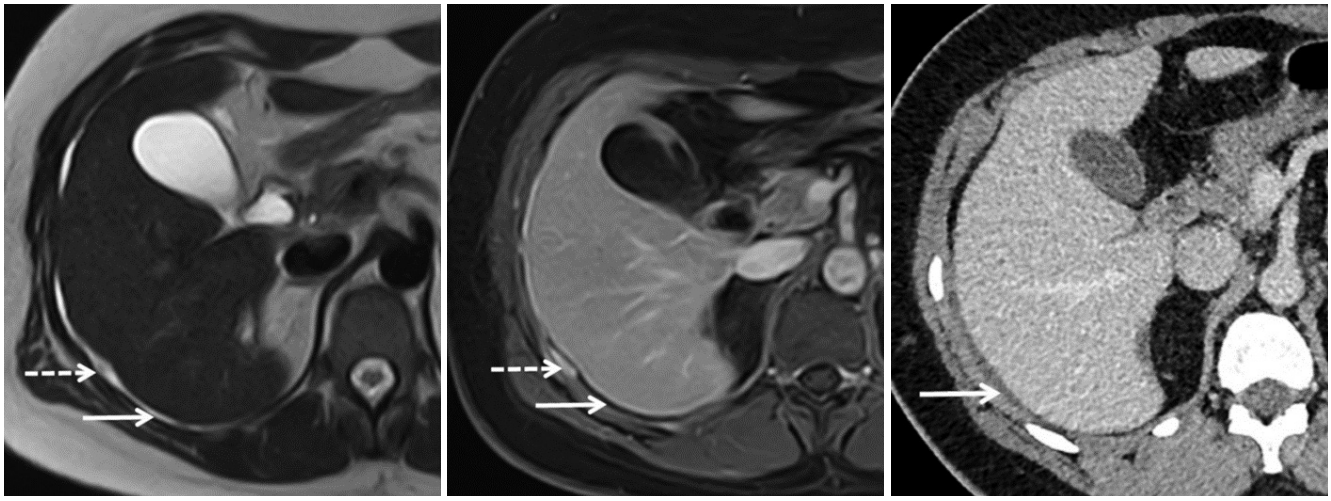

A B C

Fig. 7. Mucinous perihepatic implants of pseudomyxoma peritonei of appendicular origin.
A 35-year-old female patient with low-grade pseudomyxoma peritonei of an appendicular origin. MR images (axial T2 **(A)** and fat-suppressed gadolinium-enhanced T1-weighted **(B)**) better depict the mucinous lesions than CT **(C)** (arrows, **A, B,** and **C**). Moreover, MRI allows the characterization of the mucinous implants, which enhance (dotted arrow, **B**) and display intermediate signal intensity (dotted arrow, **A**) versus amorphous mucinous ascites, which do not enhance and display a fluid-like signal (arrows, **A, B**).

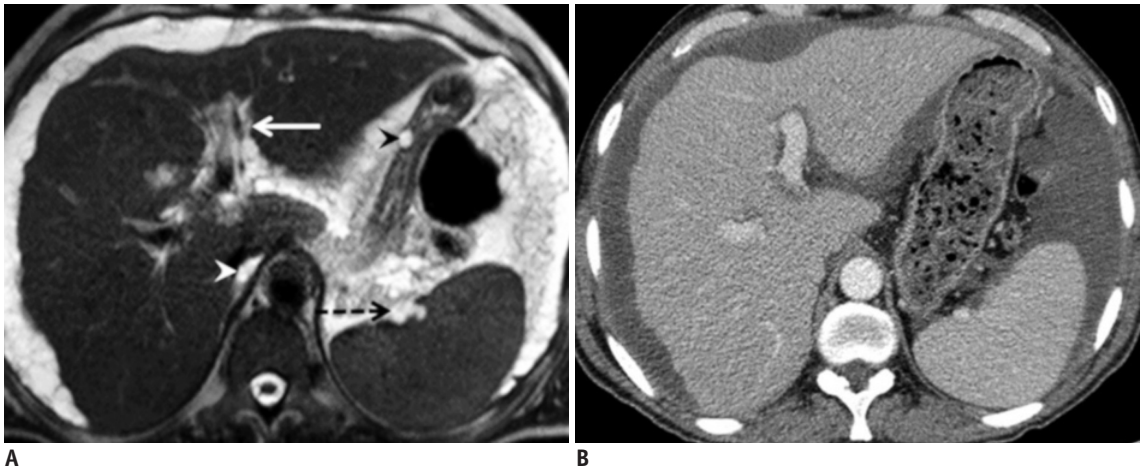

A B

Fig. 8. Better depiction of small mucinous implants using MRI than with CT.
A 65-year-old male patient with high-grade pseudomyxoma peritonei of appendicular origin. Detection and localization of the mucinous peritoneal lesions are best performed on axial T2-weighted MRI **(A)** rather than axial contrast-enhanced CT image **(B)**. Of note are the small implants seen on the wall of the lesser curvature of the stomach (black arrowhead, **A**), behind the inferior vena cava (white arrowhead, **A**), along the left portal vein (arrow, **A**), and in the splenic hilum (dotted arrow, **A**).

https://doi.org/10.3348/kjr.2019.0774

splenectomy, potentially leaving behind some fragments of the spleen. Splenosis can be spread by a capsular or intrahepatic extension (Fig. 10). MRI patterns of a single well-defined mass, which is similar to that of healthy spleen parenchyma on all sequences, along with a relevant history, should allow the diagnosis (27).

Fitz-Hugh-Curtis Syndrome

Fitz-Hugh-Curtis syndrome is frequently caused by Neisseria gonorrhoeae or Chlamydia trachomatis infections and have been reported as occurring in up to 59% of patients with pelvic inflammatory disease. It presents as a hepatic capsular and subcapsular enhancement after contrast medium intravenous administration, predominantly seen along the right antero-inferior hepatic surface on post-contrast arterial-phase CT or MRI (Fig. 11) (28, 29) due to inflammation of the hepatic capsule and edema. The diagnosis can be confirmed by laparoscopy, which allows visualization of the classic adhesions resembling violin strings and isolating the infectious agent responsible for the pelvic disease.

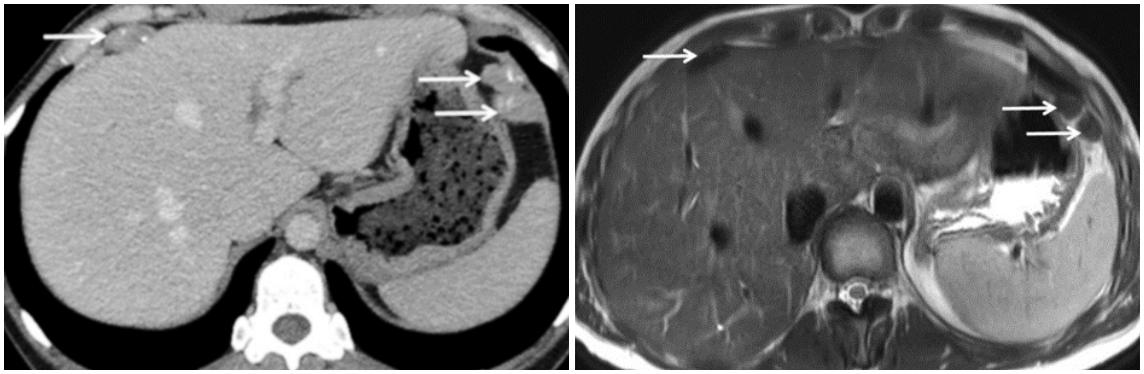

Fig. 9. Peritoneal fibromatosis in a 37-year-old female with abdominal pain. A 37-year-old female patient with a history of peritoneal fibromatosis operated on at the age of five with complete cytoreduction complaining of abdominal pain.
A. Axial contrast-enhanced CT image displays well-delineated peritoneal nodules containing calcifications, one of which is in the perihepatic space (arrows). **B.** Axial T2-weighted MR image reveals the fibrous nature of the nodules displaying low signal intensity (arrows).

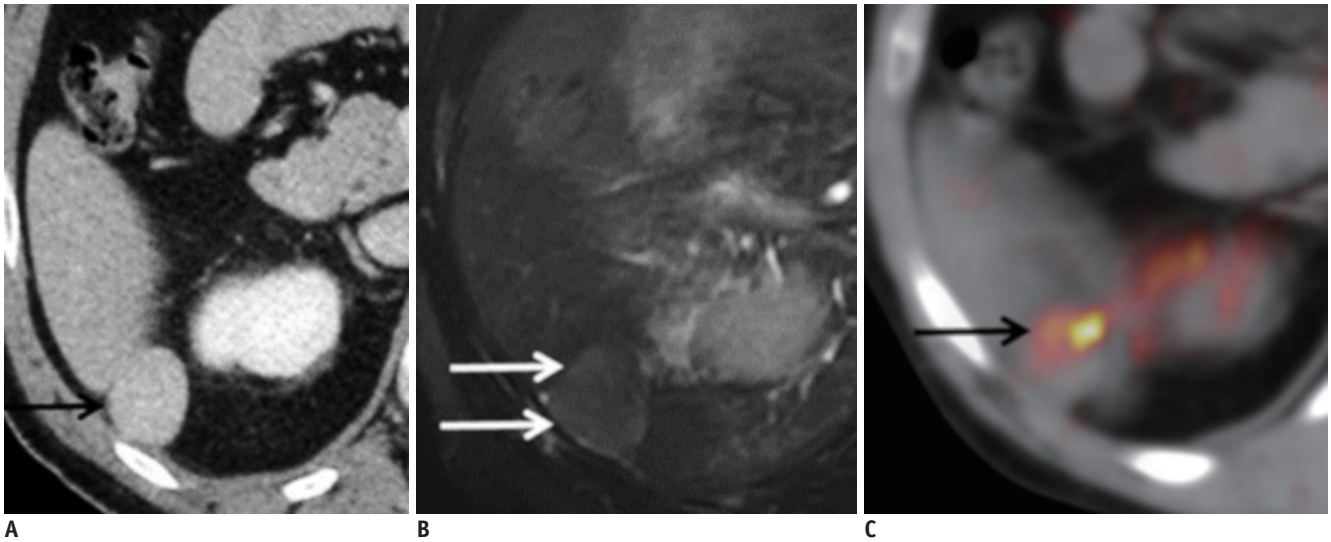

Fig. 10. MRI characteristics can make the diagnosis of splenosis.
A 53-year-old male, with a vehicle-accident history with subsequent surgical removal of the spleen some years ago. A liver lesion was fortuitously discovered. Axial **(A)** CT images obtained at a portal phase after contrast medium injection shows a rounded, well-defined, homogeneous, subhepatic lesion that seems to be extrahepatic, similar to liver parenchyma on this phase (arrow). Axial fat-suppressed T2-weighted **(B)**, as well as fat-suppressed gadolinium-enhanced T1-weighted MR images at different phases (not shown)confirm the extrahepatic location of the lesion (arrows). The lesion displays mild hyperintensity to the liver on **(B)**, slightly higher enhancement on portal phase, and lower enhancement on late phase. Red blood cell scintigraphy **(C)** confirms the diagnosis of perihepatic splenosis (arrow).

https://doi.org/10.3348/kjr.2019.0774

Korean Journal of Radiology
KJR

Endometriosis

Endometriosis may involve the diaphragm in approximately 1.5% of cases, and is symptomatic in nearly half of the cases (30). Pelvic endometriosis is almost always present. The hypothesized mechanism is that of retrograde menstruation of endometrial cells through the fallopian tubes with a clockwise peritoneal circulation through the right paracolic gutter towards the ipsilateral subdiaphragmatic area due to negative subdiaphragmatic pressure. Abdominal and liver MRI, including coronal fat-suppressed T1-weighted sequences, is the best imaging technique for diagnosing diaphragmatic endometriosis (31). Rousset et al. (30), in a series of 23 women with confirmed diaphragmatic endometriosis, showed a sensitivity of MRI of up to 83% for the detection of abnormalities in the perihepatic space. Lesions were mostly posterior nodules, although plaques and micronodular clustered lesions could also be found. The strength of the perihepatic endometriosis signal depends on the age of the lesions. Implants are typically hyperintense on T1-weighted and hypointense on T2-weighted MRI sequences (Figs. 12, 13) (32).

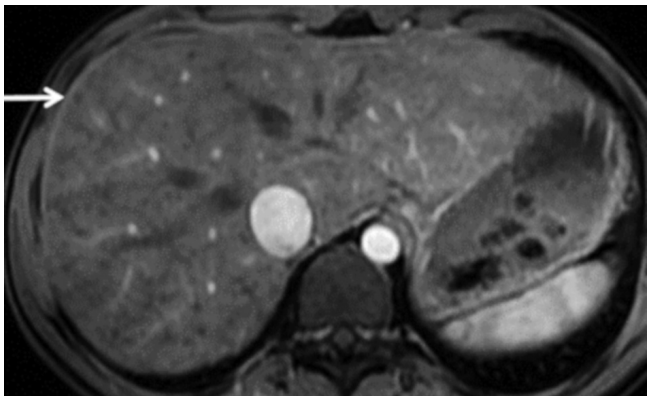

Fig. 11. Fitz-Hugh-Curtis syndrome. A 30-year-old female patient with abdominal pain and documented pelvic infection (Chlamydia trachomatis). Axial fat-suppressed gadolinium-enhanced T1-weighted MRI acquired at an arterial phase shows mild capsular perihepatic enhancement (arrow). Laparoscopy confirmed the presence of perihepatic adhesions typical of Fitz-Hugh-Curtis syndrome.

Intraperitoneal Focal Fat Infarction

Intraperitoneal focal fat infarctions include processes ranging from torsion of an epiploic appendage to infarction of the greater omentum. They may thus be found in the perihepatic space, mainly as a result of torsion of an epiploic appendage or omental infarction (33). Acute abdominal pain is the most common symptom. Differentiation between omental infarction and intraperitoneal focal fat infarction relies on the value of maximal diameter, the presence of a peripheral rim-like region, and the central dot sign. Of note, the post-infarction appendage can detach and wander around in the peritoneal

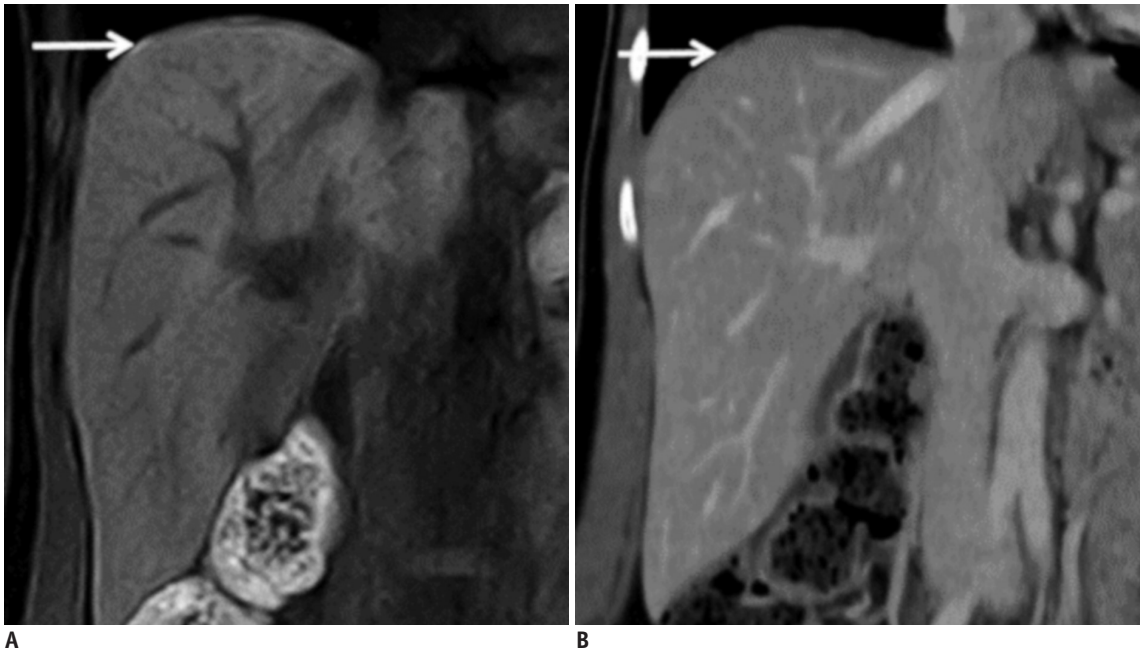

A B

Fig. 12. Endometriosis of the right subphrenic space.
A 28-year-old female patient followed-up for severe endometriosis and presenting with pain in the upper right quadrant and in the scapula during menstruation. Coronal T1-weighted MRI (arrow, **A**) optimally detects high-signal intensity, diffuse deposits on the right diaphragmatic cupola. However, on the corresponding coronal contrast-enhanced CT acquired at a portal phase (arrow, **B**), the diaphragmatic lesion is not visible. Furthermore, characterization of the lesions is not possible with CT based on their appearance.

https://doi.org/10.3348/kjr.2019.0774

cavity, covered by a fibrous capsule. It may even become lodged between the diaphragm and the superior surface of the liver (34), often on Glisson's capsule. MRI optimally depicts the fat content of these well-circumscribed small lesions and may show signal loss on opposed phased gradient-echo MRI (Fig. 14).

CONCLUSION

The perihepatic space is frequently involved by a whole

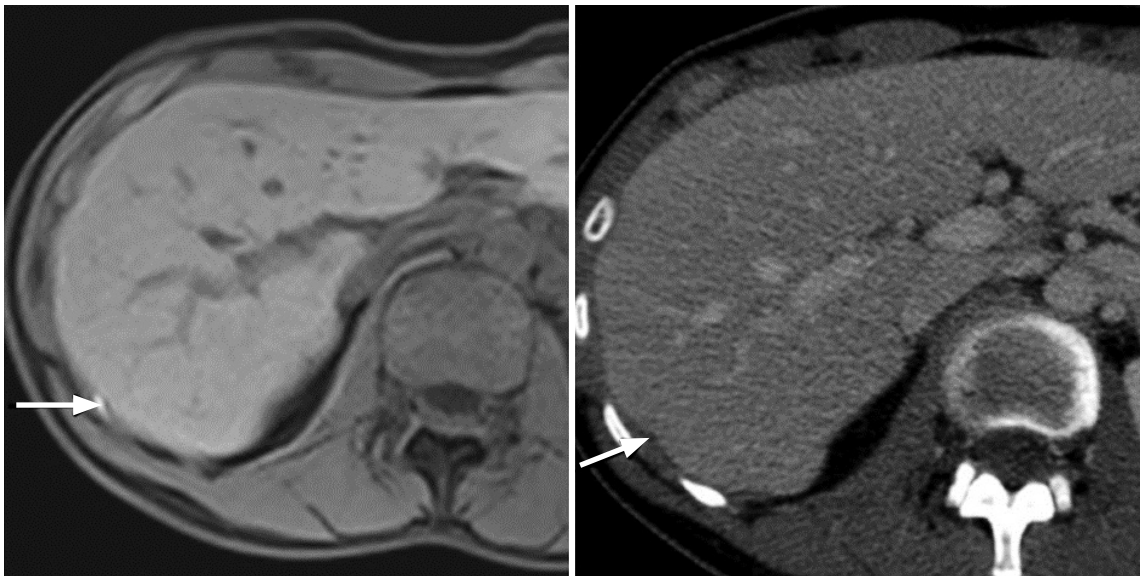

Fig. 13. MRI is the best imaging technique for the diagnosis of endometriosis.
A 32-year-old female was presenting with isolated unexplained lower thoracic pain which started seven years ago. Axial fat-suppressed abdominal T1-weighted MRI **(A)** detects a small posterolateral implant between the diaphragm and the liver, displaying a high signal intensity and suggesting endometriosis (arrow). The corresponding contrast-enhanced axial CT image **(B)** displays a non-specific hypoattenuating focus, only visible in retrospect (arrow). The radiologist interviewed the patient after the MRI, and she confirmed the catamenial nature of her thoracic pain. Three implants were seen during laparoscopy, and the diagnosis of perihepatic endometriosis was confirmed.

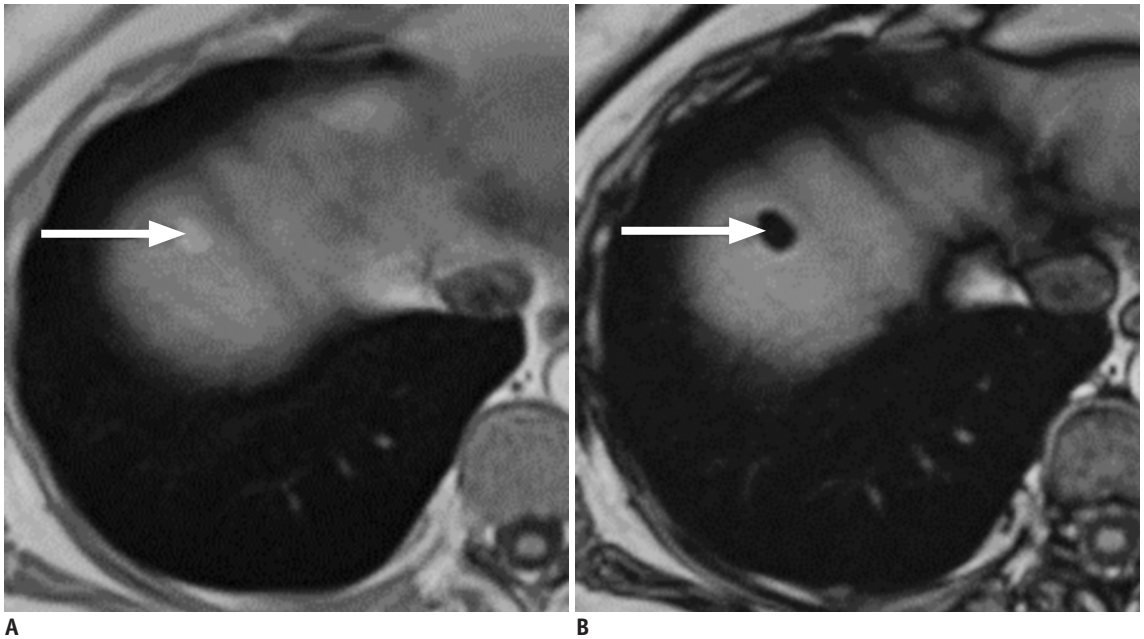

Fig. 14. Pseudolipoma of Glisson's capsule.
Axial in **(A)** and out-of-phase **(B)** MRI sequences show a small, subcapsular, well-circumscribed lesion (arrows) displaying high signal intensity on the in-phase and signal drop on the out-of-phase sequence, suggestive of fatty content.

https://doi.org/10.3348/kjr.2019.0774

Korean Journal of Radiology
KJR

spectrum of diseases. The first objective of the radiological analysis is to confirm the perihepatic origin of the lesion. The identification of the nature of the lesion then relies on both CT and MRI features and clinical presentation. Detection of the extent of the disease and identification of its nature is optimally performed with MRI, particularly for infectious entities such as stone-related perihepatic abscesses, echinococcosis, perihepatic carcinomatosis, PMP, and perihepatic endometriosis.

Radiologists should thus be familiar with abnormal MRI features of the perihepatic space and be aware of the potential role and added value of this imaging technique in the evaluation of the perihepatic space.

Supplementary Materials

The Data Supplement is available with this article at https://doi.org/10.3348/kjr.2019.0774.

Supplementary Video Legends

Video 1. Perihepatic spaces

Coronary ligaments (in blue) attach the liver to the diaphragm and merge to form the triangular ligaments (green triangles). Morison pouch (purple arrow) corresponds to the posterior subhepatic space. Subphrenic space is divided into right (pink) and left spaces (orange). Coronal T2-weighted MR images shows the spread of peritoneal disease proceeding in a clockwise direction through the right paracolic gutter to the Morrison's pouch (purple) and the right subphrenic space (pink). Right subphrenic disease can spread to the left subphrenic space and the anterior wall (orange).

Video 2. Determine intra versus perihepatic origin.

An animated picture demonstrates the key points to determine the origin intra versus perihepatic of a lesion with the example below.

In the first coronal fat-suppressed gadolinium-enhanced T1-weighted image obtained in a 48-year-old female treated for breast cancer, a peripherally-enhancing lesion is seen (in blue). This lesion is separated from the liver by a fat layer (yellow), indicating the extrahepatic origin of the lesion. Pathological examination diagnosed schwannoma of the lesser omentum.

In the coronal contrast-enhanced CT acquired at a late arterial phase obtained in a 55-year-old female with focal nodular hyperplasia (second image), the tumor (in blue) is vascularized by a hepatic artery (red), suggesting the hepatic origin of the lesion. In the last axial T2-weighted MRI image obtained in a 20-year-old female with an adrenocortical adenocarcinoma, the lesion (in blue) compresses the liver and displaces the inferior vena cava (red) anteriorly and clockwise (arrow), indicating the extra-hepatic origin of this mass.

Conflicts of Interest

The authors have no potential conflicts of interest to disclose.

ORCID iDs

Angèle Bonnin
https://orcid.org/0000-0003-0095-1060
Carole Durot
https://orcid.org/0000-0001-9293-2312
Manel Djelouah
https://orcid.org/0000-0003-0638-4415
Anthony Dohan
https://orcid.org/0000-0002-8732-5603
Lionel Arrivé
https://orcid.org/0000-0002-6184-6013
Pascal Rousset
https://orcid.org/0000-0001-6956-2800
Christine Hoeffel
https://orcid.org/0000-0002-2551-3545

REFERENCES

1. Kim S, Kim TU, Lee JW, Lee TH, Lee SH, Jeon TY, et al. The perihepatic space: comprehensive anatomy and CT features of pathologic conditions. *Radiographics* 2007;27:129-143
2. Tirkes T, Sandrasegaran K, Patel AA, Hollar MA, Tejada JG, Tann M, et al. Peritoneal and retroperitoneal anatomy and its relevance for cross-sectional imaging. *Radiographics* 2012;32:437-451
3. DeMeo JH, Fulcher AS, Austin RF Jr. Anatomic CT demonstration of the peritoneal spaces, ligaments, and mesenteries: normal and pathologic processes. *Radiographics* 1995;15:755-770
4. Patel CM, Sahdev A, Reznek RH. CT, MRI and PET imaging in peritoneal malignancy. *Cancer Imaging* 2011;11:123-139
5. Oh SN, Rha SE, Byun JY, Kim JY, Song KY, Park CH. Chilaiditi syndrome caused by Fitz-Hugh-Curtis syndrome: multidetector CT findings. *Abdom Imaging* 2006;31:45-47
6. Mulé S, Colosio A, Cazejust J, Kianmanesh R, Soyer P, Hoeffel C. Imaging of the postoperative liver: review of normal appearances and common complications. *Abdom Imaging*

2015;40:2761-2776
7. Lee NK, Kim S, Lee JW, Lee SH, Kang DH, Kim GH, et al. Biliary MR imaging with Gd-EOB-DTPA and its clinical applications. *Radiographics* 2009;29:1707-1724
8. Ciolina M, Di Martino M, Bruno O, Pommier R, Vilgrain V, Ronot M. Peritoneal and pleural fluids may appear hyperintense on hepatobiliary phase using hepatobiliary MR contrast agents. *Eur Radiol* 2018;28:3020-3031
9. Dhaka N, Samanta J, Kochhar S, Kalra N, Appasani S, Manrai M, et al. Pancreatic fluid collections: what is the ideal imaging technique? *World J Gastroenterol* 2015;21:13403-13410
10. Huh J, Kim SY, Yeh BM, Lee SS, Kim KW, Wu EH, et al. Troubleshooting arterial-phase MR images of gadoxetate disodium-enhanced liver. *Korean J Radiol* 2015;16:1207-1215
11. Foster BR, Jensen KK, Bakis G, Shaaban AM, Coakley FV. Revised Atlanta classification for acute pancreatitis: a pictorial essay. *Radiographics* 2016;36:675-687
12. Tonolini M, Ierardi AM, Patella F, Carrafiello G. Early cross-sectional imaging following open and laparoscopic cholecystectomy: a primer for radiologists. *Insights Imaging* 2018;9:925-941
13. Black MT, Ha BY, Kang YS, Garland AM. Perihepatic abscess caused by dropped appendicoliths following laparoscopic appendectomy: sonographic findings. *J Clin Ultrasound* 2013;41:366-369
14. Nayak L, Menias CO, Gayer G. Dropped gallstones: spectrum of imaging findings, complications and diagnostic pitfalls. *Br J Radiol* 2013;86:e20120588
15. Kantarci M, Bayraktutan U, Karabulut N, Aydinli B, Ogul H, Yuce I, et al. Alveolar echinococcosis: spectrum of findings at cross-sectional imaging. *Radiographics* 2012;32:2053-2070
16. Kodama Y, Fujita N, Shimizu T, Endo H, Nambu T, Sato N, et al. Alveolar echinococcosis: MR findings in the liver. *Radiology* 2003;228:172-177
17. Bulakçı M, Kartal MG, Yılmaz S, Yılmaz E, Yılmaz R, Şahin D, et al. Multimodality imaging in diagnosis and management of alveolar echinococcosis: an update. *Diagn Interv Radiol* 2016;22:247-256
18. Beaussant-Cohen S, Richou C, Lenoir M, Grenouillet F, Bresson-Hadni S, Delabrousse E. MR imaging features of peritoneal alveolar echinococcosis. *Diagn Interv Imaging* 2018;99:511-512
19. Kim HJ, Byun JH, Kim DY, Won HJ, Shin YM, Ha HK. Isolated perihepatic tuberculosis: imaging findings. *Clin Radiol* 2009;64:184-189
20. Low RN, Barone RM, Lucero J. Comparison of MRI and CT for predicting the Peritoneal Cancer Index (PCI) preoperatively in patients being considered for cytoreductive surgical procedures. *Ann Surg Oncol* 2015;22:1708-1715
21. Nougaret S, Addley HC, Colombo PE, Fujii S, Al Sharif SS, Tirumani SH, et al. Ovarian carcinomatosis: how the radiologist can help plan the surgical approach. *Radiographics* 2012;32:1775-1800
22. Dohan A, Hoeffel C, Soyer P, Jannot AS, Valette PJ, Thivolet A, et al. Evaluation of the peritoneal carcinomatosis index with CT and MRI. *Br J Surg* 2017;104:1244-1249
23. Low RN, Sebrechts CP, Barone RM, Muller W. Diffusion-weighted MRI of peritoneal tumors: comparison with conventional MRI and surgical and histopathologic findings--a feasibility study. *AJR Am J Roentgenol* 2009;193:461-470
24. Low RN, Barone RM. Combined diffusion-weighted and gadolinium-enhanced MRI can accurately predict the peritoneal cancer index preoperatively in patients being considered for cytoreductive surgical procedures. *Ann Surg Oncol* 2012;19:1394-1401
25. Menassel B, Duclos A, Passot G, Dohan A, Payet C, Isaac S, et al. Preoperative CT and MRI prediction of non-resectability in patients treated for pseudomyxoma peritonei from mucinous appendiceal neoplasms. *Eur J Surg Oncol* 2016;42:558-566
26. Al-Talib A, Tulandi T. Pathophysiology and possible iatrogenic cause of leiomyomatosis peritonealis disseminata. *Gynecol Obstet Invest* 2010;69:239-244
27. Pandey A, Pandey P, Ghasabeh MA, Varzaneh FN, Khoshpouri P, Shao N, et al. Accuracy of apparent diffusion coefficient in differentiating pancreatic neuroendocrine tumour from intrapancreatic accessory spleen. *Eur Radiol* 2018;28:1560-1567
28. Kim JY, Kim Y, Jeong WK, Song SY, Cho OK. Perihepatitis with pelvic inflammatory disease (PID) on MDCT: characteristic findings and relevance to PID. *Abdom Imaging* 2009;34:737-742
29. Czeyda-Pommersheim F, Kalb B, Costello J, Liau J, Meshksar A, Arif Tiwari H, et al. MRI in pelvic inflammatory disease: a pictorial review. *Abdom Radiol (NY)* 2017;42:935-950
30. Rousset P, Gregory J, Rousset-Jablonski C, Hugon-Rodin J, Regnard JF, Chapron C, et al. MR diagnosis of diaphragmatic endometriosis. *Eur Radiol* 2016;26:3968-3977
31. Beranger-Gibert S, Lagadec M, Boulay-Coletta I, Petit E, Barrau V, Zins M, et al. Hepatic and perihepatic involvement of female genital diseases and pregnancy: a review. *Abdom Imaging* 2015;40:1331-1349
32. Rousset P, Rousset-Jablonski C, Alifano M, Mansuet-Lupo A, Buy JN, Revel MP. Thoracic endometriosis syndrome: CT and MRI features. *Clin Radiol* 2014;69:323-330
33. Eberhardt SC, Strickland CD, Epstein KN. Radiology of epiploic appendages: acute appendagitis, post-infarcted appendages, and imaging natural history. *Abdom Radiol (NY)* 2016;41:1653-1665
34. Prasad SR, Wang H, Rosas H, Menias CO, Narra VR, Middleton WD, et al. Fat-containing lesions of the liver: radiologic-pathologic correlation. *Radiographics* 2005;25:321-331

https://doi.org/10.3348/kjr.2019.0774